

Characteristics of PMN-PZT ferroelectric electron emitters with three-dimensional emission sites formed by chemical etching

Tomohiko Sugiyama, Iwao Ohwada, Tsutomu Nanataki, Yukihisa Moriguchi, Osamu Eryu et al.

Citation: *J. Vac. Sci. Technol. B* **29**, 032210 (2011); doi: 10.1116/1.3592993

View online: <http://dx.doi.org/10.1116/1.3592993>

View Table of Contents: <http://avspublications.org/resource/1/JVTBD9/v29/i3>

Published by the AVS: Science & Technology of Materials, Interfaces, and Processing

Related Articles

Observation of fringelike electron emission pattern from triode Pt nano electron source fabricated by electron-beam-induced deposition

J. Vac. Sci. Technol. B **31**, 02B107 (2013)

X-ray tube with a graphite field emitter inflated at high temperature

J. Vac. Sci. Technol. B **31**, 02B106 (2013)

Improved approach to Fowler–Nordheim plot analysis

J. Vac. Sci. Technol. B **31**, 02B103 (2013)

Illustrating field emission theory by using Lauritsen plots of transmission probability and barrier strength

J. Vac. Sci. Technol. B **31**, 02B102 (2013)

Experimental study of electric field screening by the proximity of two carbon fiber cathodes

J. Vac. Sci. Technol. B **30**, 061803 (2012)

Additional information on *J. Vac. Sci. Technol. B*

Journal Homepage: <http://avspublications.org/jvstb>

Journal Information: http://avspublications.org/jvstb/about/about_the_journal

Top downloads: http://avspublications.org/jvstb/top_20_most_downloaded

Information for Authors: http://avspublications.org/jvstb/authors/information_for_contributors

ADVERTISEMENT

Instruments for advanced science

Gas Analysis



- dynamic measurement of reaction gas streams
- catalysis and thermal analysis
- molecular beam studies
- dissolved species probes
- fermentation, environmental and ecological studies

Surface Science



- UHV TPD
- SIMS
- end point detection in ion beam etch
- elemental imaging - surface mapping

Plasma Diagnostics



- plasma source characterization
- etch and deposition process reaction kinetic studies
- analysis of neutral and radical species

Vacuum Analysis



- partial pressure measurement and control of process gases
- reactive sputter process control
- vacuum diagnostics
- vacuum coating process monitoring

contact Hiden Analytical for further details

HIDEN ANALYTICAL

info@hideninc.com
www.HidenAnalytical.com

CLICK to view our product catalogue 

Characteristics of PMN-PZT ferroelectric electron emitters with three-dimensional emission sites formed by chemical etching

Tomohiko Sugiyama,^{a)} Iwao Ohwada, and Tsutomu Nanataki
Corporate R&D, NGK Insulators, Ltd., Nagoya 467-8530, Japan

Yukihisa Moriguchi, Osamu Eryu, Masaya Ichimura, and Manabu Gomi
Nagoya Institute of Technology, Nagoya 466-8555, Japan

(Received 19 October 2010; accepted 30 April 2011; published 26 May 2011)

$\text{Pb}(\text{Mg}_{1/3}\text{N}_{2/3})\text{O}_3\text{-PbZrO}_3\text{-PbTiO}_3$ (PMN-PZT) ferroelectric electron emitters with a novel electrode structures were formed by photolithography and chemical etching to investigate their electron emission characteristics. For the electron emitter formed with the most suitable etching time, the electron emission density was 17 nC/cm^2 . An electric potential distribution was simulated to clarify the effects of the vacuum gap, and results confirmed that the vacuum gap produces an electric field that leads electrons from the ferroelectric surface to the surrounding space. © 2011 American Vacuum Society. [DOI: 10.1116/1.3592993]

I. INTRODUCTION

Ferroelectric materials have attracted significant attention because electrons can be efficiently emitted from their surface without requiring a high electric field. Many kinds of ferroelectric crystals and ceramics have been utilized for this purpose.¹ Recently, it has been reported that electron emission from $[\text{Pb}(\text{Mg}_{1/3}\text{Nb}_{2/3})\text{O}_3]_{0.72}\text{-}[\text{PbTiO}_3]_{0.28}$ ferroelectric single crystals emit electrons at low voltages.² The following are the two types of electron emission that have been reported: (1) electron emission due to the repulsion between surface screening electrons on a ferroelectric layer when surface polarization is switched from positive to negative,³⁻⁷ and (2) electron emission from a surface plasma on a ferroelectric layer, which involves the flow of a large number of electrons upon the spontaneous polarization of the ferroelectric medium.⁶⁻⁹

For a conventional electron emitter using a ferroelectric layer, a comb-like electrode with openings for electron emission is generally used. Recently, Ohwada and colleagues have observed that electrons are emitted from the surface of a ferroelectric thick film with numerous microopenings on the electrode and “vacuum gaps” between the electrode and the surface of the ferroelectric layer.¹⁰⁻¹² The vacuum gaps mentioned in Ref. 1 were parallel to the ferroelectric surface, and differed from those discussed in this article. The structure of the ferroelectric electron emitter was formed by screen printing and firing from bottom to top onto a zirconia substrate.¹¹ Electrons were emitted from the entire surface of the emitter during a positive polarization reversal, which was attributed to the electron emission caused by the switch in surface polarization. Ohwada *et al.* proposed, on the basis of detailed experiments, that electrons are emitted through the following two processes:^{11,12}

Process (1): Electrons diffuse on an electrodeless ferroelectric surface from the electrode and compensate the

polarized charge (the ferroelectric surface becomes positively poled).

Process (2): Screening electrons are emitted by Coulomb repulsion when the polarization is reversed (the ferroelectric surface becomes negatively poled).

In process (2), it has been confirmed that the vacuum gap promotes electron emission.¹¹ Therefore, optimizing the shape of the vacuum gap is important for obtaining a large electron emission density. However, control of the structure of the electron-emitting portion has been limited because the electrode structures have typically been automatically formed by sintering.

In this study, we have investigated electron emission from a novel electrode structure with a vacuum gap, formed using photolithography and chemical etching. Furthermore, we have determined the relationship between the formed vacuum gap and its electron emission.

II. EXPERIMENTAL PROCEDURE

Figure 1 shows the sequence of processes involved in forming the ferroelectric electron emitter. First, a lower electrode and a ferroelectric layer are formed by screen printing and firing onto a zirconia substrate (Fig. 1(a)). The ferroelectric material is a ternary system of $\text{Pb}(\text{Mg}_{1/3}\text{N}_{2/3})\text{O}_3\text{-PbZrO}_3\text{-PbTiO}_3$ (PMN-PZT), and the thickness of the ferroelectric layer is $20 \mu\text{m}$. Then, the ferroelectric surface is planarized by chemical mechanical polishing (Fig. 1(b)). The upper electrode of the sputtered Pt thin film with dot pattern openings is formed by photolithography and a liftoff process (Fig. 1(c)). Dot pattern openings are $10 \mu\text{m}$ in diameter with a $10 \mu\text{m}$ spaces between each opening. They are arranged in a 150×300 matrix over a $3.0 \times 6.0 \text{ mm}^2$ area. The sample is annealed in oxygen at $500 \text{ }^\circ\text{C}$ to increase adhesion. The sample is etched to form a vacuum gap at the edge of an electrode opening (Fig. 1(d)). The etching solution used is composed of 0.045 wt % HF, 2.21 wt % HNO_3 , 15.60 wt % H_2O_2 , and 82.145 wt % H_2O . The Pt upper electrode is not etched; only the ferroelectric layer in the electrode opening is

^{a)}Electronic mail: tom-sugi@ngk.co.jp

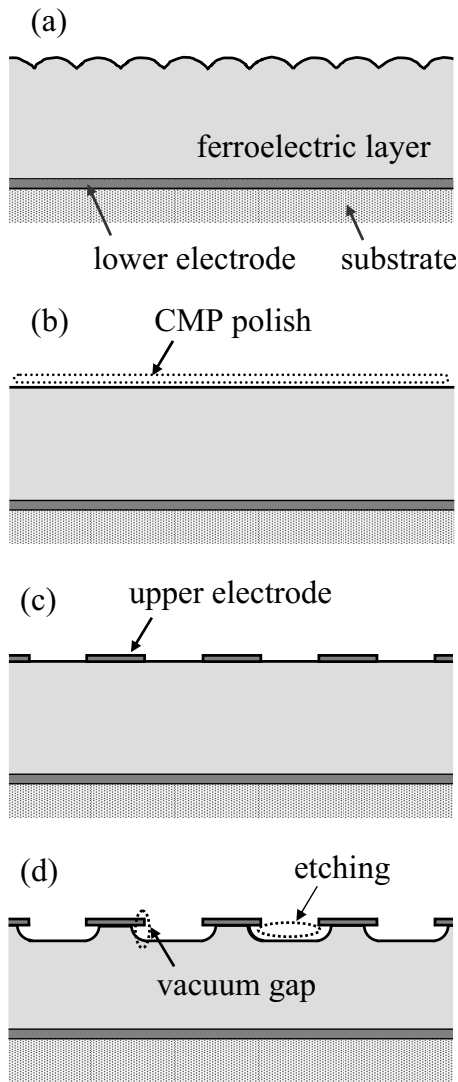


FIG. 1. Sequence of processes involved in forming ferroelectric electron emitter. (a) Formation of lower electrode and ferroelectric layer by screen printing and firing onto zirconia substrate. (b) Planarization of ferroelectric surface by chemical mechanical polishing. (c) Formation of upper electrode of sputtered Pt thin film with dot pattern openings. (d) Etching to form vacuum gap at edge of electrode opening.

etched. The size of the vacuum gap is controlled by changing the etching time.

Figure 2 shows the experimental setup, which is the same as that used in previous studies.^{11,12} The chamber into which the electron emitter was inserted was evacuated to a pressure of up to 10^{-3} Pa. A drive voltage with a square waveform (100 Hz) comprising a 300 V negative component and a 50 V positive component was applied to the lower electrode of the electron emitter via a series resistance of 10 k Ω . The emitted electrons were collected by applying a voltage of 3 kV between the upper electrode (ground) and a collector electrode located 5 mm from the electron emitter. The electron emission density, excluding the electrons absorbed by the upper electrode, was obtained by integrating the collector current. The polarization curve of the ferroelectric layer was

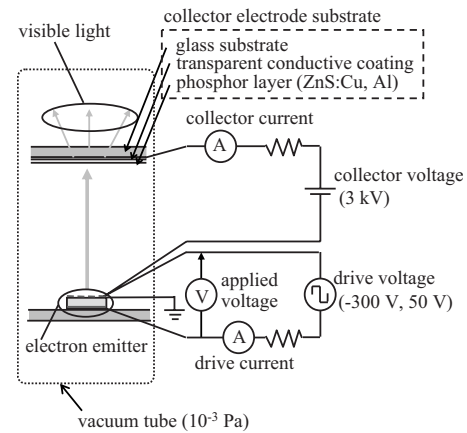


FIG. 2. Schematic illustration of experimental setup for measuring electron emission, which is the same as that in previous studies.^{11,12}

estimated using the applied voltage and the remnant polarization (2Pr), which was obtained by integrating the drive current.

To examine the effect of the formed vacuum gap on electron emission, the electron field near the vacuum gap was simulated. The simulator used was “ELFIN,” developed by ELF Corporation. The relative permittivity of the ferroelectric material was set to 2000.

III. RESULTS AND DISCUSSION

Figure 3 shows a top view of a sample. To observe the formed vacuum gap, the focused ion beam (FIB) process was used, as shown in Fig. 3. Figure 4 shows oblique cross-sectional views of the regions near the upper electrode openings of samples etched for 0, 2, 4, and 6 min. For the etched samples, the vacuum gap was formed around the edge of the upper electrode. The sizes of the vacuum gaps increased with etching time. Samples etched for 2, 4, and 6 min had vacuum gaps of 0.3, 0.6, and 0.9 μm , respectively, in both the vertical and horizontal directions. Figure 5 shows waveforms of voltage applied between the electrodes of the ferroelectric layer and the collector current on 4 min etched sample. The waveform of the collector current indicated that electrons were emitted when applied voltage was switched from negative to positive (the ferroelectric surface became negatively

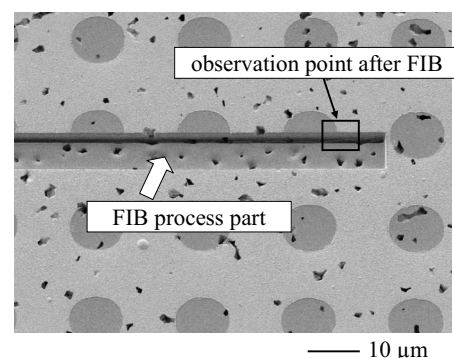


FIG. 3. Top view of sample with dot pattern openings.

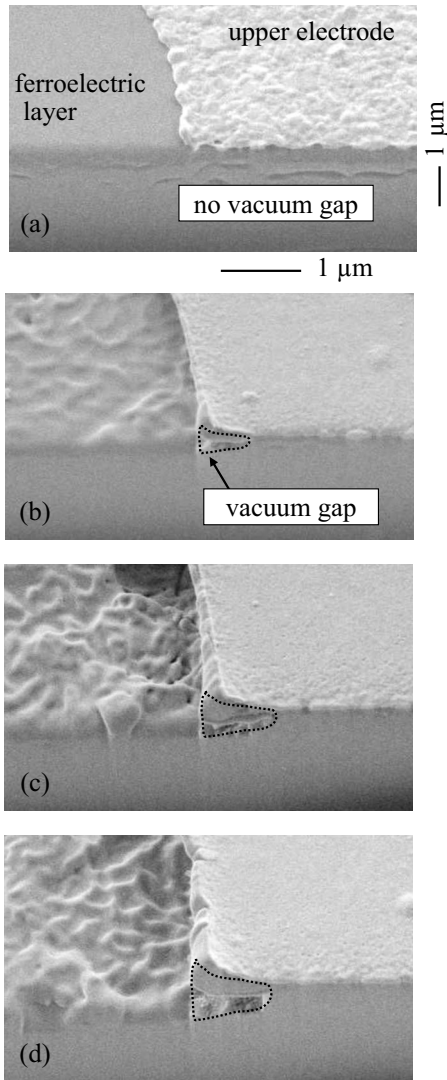


FIG. 4. Oblique cross-sectional views of (a) nonetched, (b) 2 min etched, (c) 4 min etched, and (d) 6 min etched samples. All images have the same scale.

poled). Figure 6 shows the polarization curve of each sample. The origin of the asymmetric polarization has been discussed in previous articles.^{11,12} The remnant polarization decreased with etching time. Because prolonging the etching increases the vacuum gap as shown in Fig. 3, it is assumed

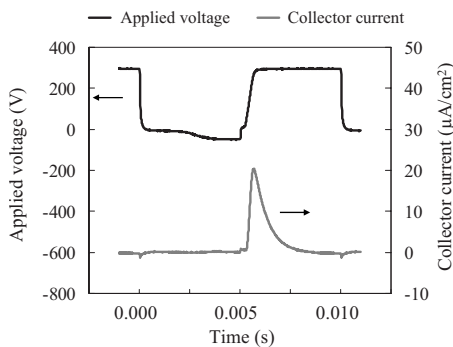


FIG. 5. Waveforms of voltage applied between the electrodes of the ferroelectric layer and the collector current on 4 min etched sample.

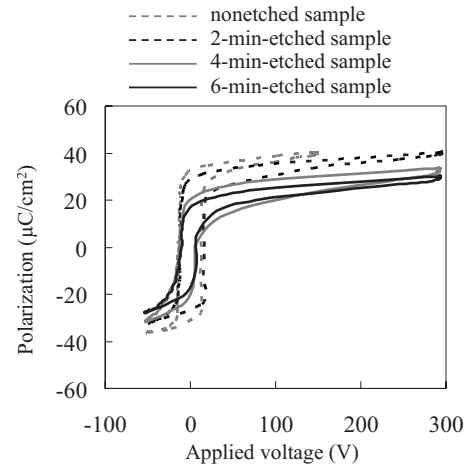


FIG. 6. Polarization curves of nonetched, 2 min etched, 4 min etched, and 6 min etched samples.

that part of the voltage applied to the electron emitter is applied to the vacuum gap. This explains why the remnant polarization decreased with etching time. Figure 7 shows the electron emission density as a function of etching time. The nonetched sample emitted very few electrons. However, electron emission was promoted by etching, and the sample etched for 4 min exhibited a maximum electron emission density of 17 nC/cm^2 , which is lower than values reported in previous studies.^{11,12} The reason for this is that the density of openings for electron emission in the upper electrode obtained by photolithography is lower than that obtained by sintering.

Figure 8 shows the simulation results of the electric potential distributions near the upper electrode openings of the nonetched and etched samples in the electron emission process. A drive voltage of -300 V was applied to the lower electrode. For the nonetched sample, the equipotential lines near the electrode opening are distributed vertically, as observed in previous studies.^{13–15} Therefore, most of the emitted electrons are absorbed by the upper electrode. On the other hand, for the etched sample, the equipotential lines near the vacuum gap are distributed horizontally. These results suggest that the vacuum gap produced an electric field that led electrons from the ferroelectric surface to the sur-

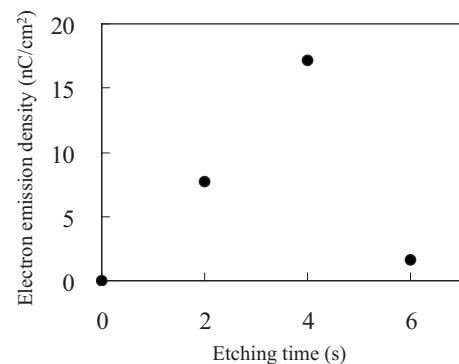


FIG. 7. Etching time versus electron emission density.

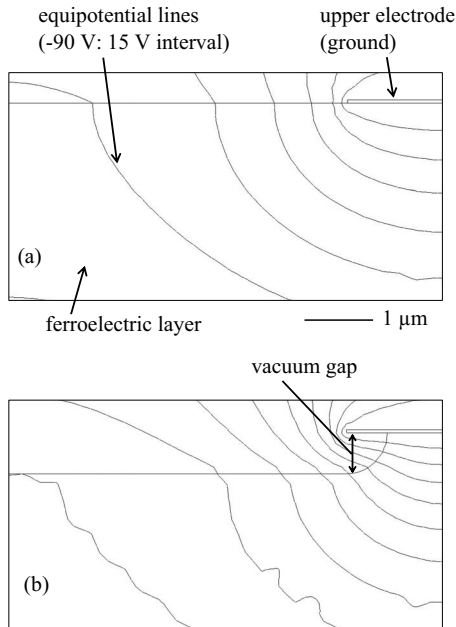


FIG. 8. Electric potential distributions near upper electrode openings of (a) nonetched sample and (b) etched samples. A drive voltage of -300 V was applied to the lower electrode. Both images have the same scale.

rounding space. However, the electron emission density of the sample etched for 6 min was lower than that of one etched for 4 min. The increase in etching time decreased the remnant polarization, due to the increase in the vacuum gap, as mentioned above. Thus, it is considered that the polarization was not reversed below the edge of the upper electrode when the vacuum gap became excessive. As a result, electrons were not come out to the surrounding space to be subjected to interference by the upper electrode. This explains why the electron emission density of the sample etched for 6 min is low. Under our experimental conditions, the vacuum gap formed by etching for 4 min was observed to be the most suitable for electron emission.

IV. CONCLUSIONS

An electron emitter with a novel electrode structure has been manufactured by photolithography and chemical etching. Control of the vacuum gap size was possible by adjusting the etching time. For the electron emitter formed with a suitable etching time, the electron emission density was 17 nC/cm². When an electric potential distribution was simulated to clarify the effects of the vacuum gap, it was confirmed that the vacuum gap produced an electric field that led electrons from the ferroelectric surface to the surrounding space. If the shape of the vacuum gap is optimized and openings in the upper electrode for electron emission are formed at a high density, the electron emission density of the ferroelectric electron emitter is expected to improve significantly.

¹G. Rosenman and D. Shur, *J. Appl. Phys.* **88**, 6109 (2000).

²O. Mieth, H. Klumbies, V. S. Vidyarthi, G. Gerlach, K. Dörr, and L. M. Eng, *New J. Phys.* **11**, 023004 (2009).

³H. Gundel, H. Riege, E. J. N. Wilson, J. Handerek, and K. Zioutas, *Ferroelectrics* **100**, 1 (1989).

⁴M. Angadi, O. Auciello, A. R. Krauss, and H. W. Gundel, *Appl. Phys. Lett.* **77**, 2659 (2000).

⁵K. Omura and S. Morita, *Jpn. J. Appl. Phys.* **43**, L689 (2004).

⁶D. N. J. Shannon, P. W. Smith, P. J. Dobson, and M. J. Shaw, *Appl. Phys. Lett.* **70**, 1625 (1997).

⁷V. F. Puchkarev and G. A. Mesyats, *J. Appl. Phys.* **78**, 5633 (1995).

⁸D. Shur, G. Rosenman, and Y. E. Krasik, *Appl. Phys. Lett.* **70**, 574 (1997).

⁹K. Yasuoka and S. Ishi, *Oyo Buturi* **68**, 546 (1999) (in Japanese).

¹⁰Y. Takeuchi, T. Nanataki, and I. Ohwada, *SID Int. Symp. Digest Tech. Papers* **36**, 1724 (2005).

¹¹I. Ohwada, T. Sugiyama, and T. Nanataki, *Jpn. J. Appl. Phys.* **46**, 1643 (2007).

¹²T. Sugiyama, I. Ohwada, T. Nanataki, O. Eryu, M. Ichimura, and M. Gomi, *J. Appl. Phys.* **107**, 114109 (2010).

¹³J. Park, Y. T. Kim, and K. H. Yoon, *J. Appl. Phys.* **91**, 1458 (2002).

¹⁴I. Boscolo and S. Cialdi, *J. Appl. Phys.* **91**, 6125 (2002).

¹⁵G. Suchanek, V. S. Vidyarthi, G. Gerlach, A. V. Solnyshkin, and I. L. Kislova, *IEEE Trans. Ultrason. Ferroelectr. Freq. Control* **54**, 2555 (2007).